Electronic Supplementary Material (ESI) for Journal of Materials Chemistry C.

A MOF/Hydrogel Film-Based Array Sensor for Discriminative Detection of Nitrophenol Isomers

Gaowei Wang [a, ⊥], Zhengluan Liao [a, ⊥], Ziwei Jiang [a], Wenqian Cao [a, b], Yu Yang [a,], Guodong Qian [a] and Yuanjing Cui [a, b, *]*

[a] *State Key Laboratory of Silicon and Advanced Semiconductor Materials, School of Materials Science & Engineering, Zhejiang University, Hangzhou 310027, China.*

[b] *ZJU-Hangzhou Global Scientific and Technological Innovation Center, Zhejiang University, Hangzhou 311215, China.*

E-mail addresses: yuyang@zju.edu.cn; cuiyj@zju.edu.cn

[⊥] *These authors contributed equally to this paper.*

1. Materials and methods.

All of the solvents and reagents in this article were purchased from commercial companies and used without further purification. Zirconium chloride, H_4btec and 1,4-NDC were purchased from Aladdin Industrial Inc. to synthesize the sensor Eu^{3+}/Tb^{3+}@Uio-66-$(COOH)_2$/NDC. The metal salts $Eu(NO_3)_3 \cdot 6H_2O$ and $Tb(NO_3)_3 \cdot 6H_2O$ were purchased from ASCENDER Chemical Technology Co., Ltd. and their solutions were prepared by dissolving the reagent in deionized water. Three nitrophenol isomers and sodium alginate were purchased from MACKLIN Biochemical Technology Co., Ltd. and their solutions were prepared by dissolving the reagent in deionized or running water. Powder X-ray diffraction (PXRD) patterns were recorded on Shimadzu XRD7000 powder X-ray diffractometer at the range of 2~50° for 2θ with Cu Kα radiation at room temperature. ^{1}H nuclear magnetic resonance (^{1}H NMR) spectra were recorded on Bruker Advance DMX 500 spectrometer using tetramethylsilane as an internal standard. Fourier transform infrared (FT-IR) spectra were characterized by ThermoFisher Nicolet iN10 spectrometer using potassium bromide pellet method. Inductively coupled plasma-mass spectrometry (ICP-MS) of the digested sample was recorded on ThermoFisher iCAP Pro X. The scanning electron microscopy (SEM) image and energy dispersive spectroscopy (EDS) pattern were carried out on Hitachi S4800 Scanning Electron Microscope equipped with EDAX TEAM. Nitrogen adsorption-desorption curves were recorded on Micromeritics ASAP 2460 surface area analyser. Thermogravimetric analyses (TGA) were tested on a Mettler-Toledo TGA/DSC3+ with a heating rate of 5 ℃·min^{-1} under a nitrogen atmosphere. The photoluminescence (PL) spectra at room temperature for different samples were performed on a Hitachi F4600 fluorescence spectrometer. Ultraviolet-visible absorption (UV-vis) spectra were performed on a Hitachi U-4100 spectrometer.

2. Calculation methods.

We use Fishe Discriminant to implement LDA analysis. The following is the the derivation of the discriminant formula:

$$H = \sum_{i=1}^{k} n_i(\bar{x}_i - \bar{x})(\bar{x}_i - \bar{x})^{'},$$

$$E = \sum_{i=1}^{k} (n_i - 1)S_i,$$

$$\bar{x}_i = \frac{1}{n_i}\sum_{j=1}^{n_i} x_{ij}, \bar{x} = \frac{1}{n}\sum_{i=1}^{k} n_i\bar{x}_i, n = \sum_{i=1}^{k} n_i, S_i = \frac{1}{n_i - 1}\sum_{j=1}^{n_i} (x_{ij} - \bar{x}_i)(x_{ij} - \bar{x}_i)^{'},$$

$$j = 1,2,3...n_i, i = 1,2...k,$$

The joint unbiased estimation of the covariance matrix Σ:

$$S_p = \frac{1}{n-k}\sum_{i=1}^{k} (n_i - 1)S_i = \frac{1}{n-k}E,$$

We suppose $\Sigma_1 = \Sigma_2 = ... = \Sigma_k = \Sigma_1$ and all positive eigenvalues λ_s of $E^{-1}H$:

$\lambda_1 \geq \lambda_2 \geq ... \geq \lambda_s \geq 0$

$s = rank(H)$

The corresponding eigenvector are $t_1, t_2, ...t_s$. Then we normalize the matrix:

$t_i^{'} S_p t_i = 1, i = 1,2,...,s$

Then the Fishe Discriminant formula is:

$y_i = t_i^{'} x, i = 1,2,...,s$

After we obtain the fluorescence intensity change value of each luminescent center, we substituted it into the JMP PRO 16 software for linear discriminant analysis and the canonical score plot was finally obtained.

3. Figure.

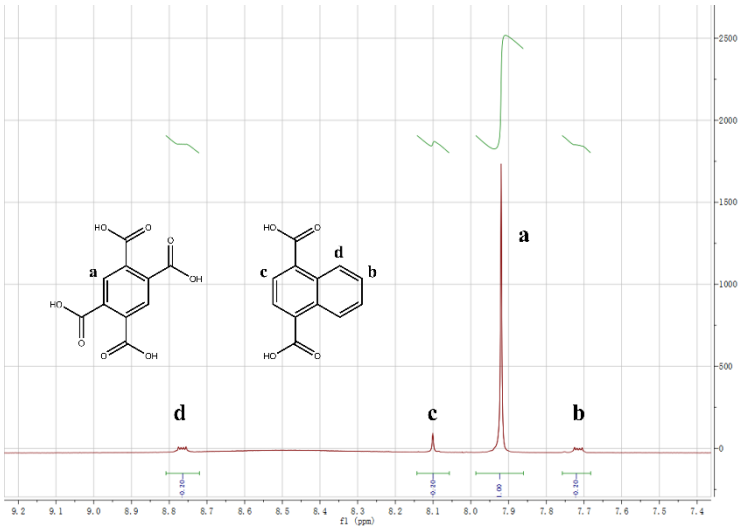

Fig. S1. ^{1}H NMR spectra of Uio-66-$(COOH)_2$/NDC dissolved in hydrofluoric acid and deuterated dimethyl sulfoxide.

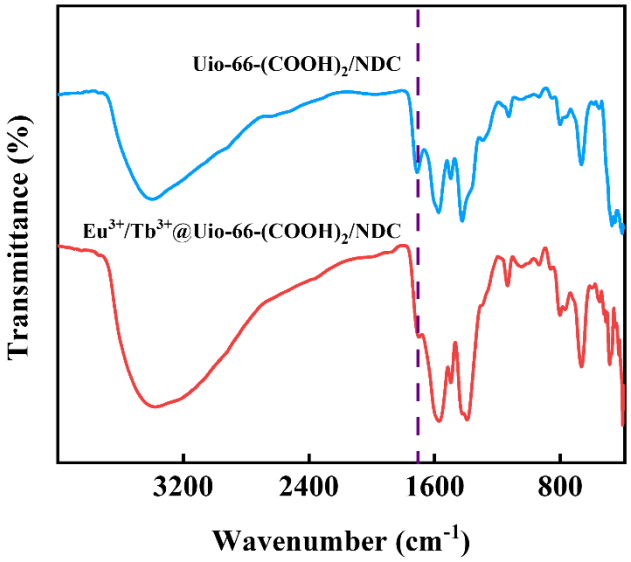

Fig. S2. FT-IR spectroscopy of Uio-66-$(COOH)_2$/NDC and Eu^{3+}/Tb^{3+}@Uio-66-$(COOH)_2$/NDC.

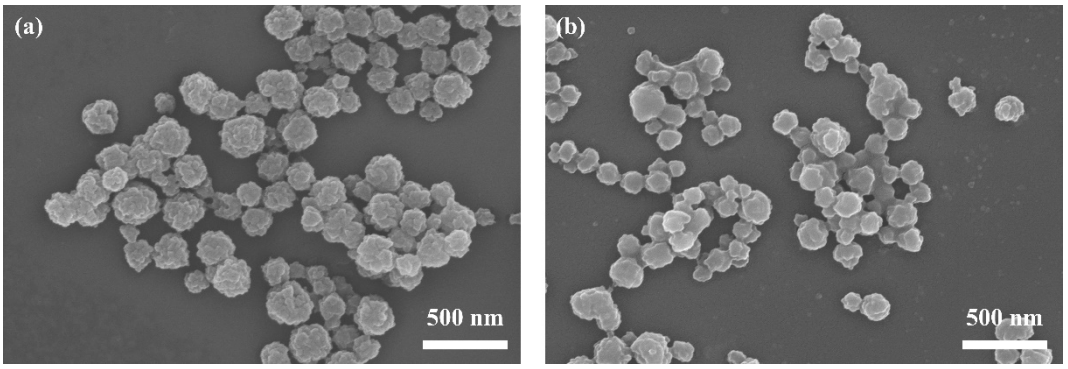

Fig. S3. SEM image of (a) Uio-66-$(COOH)_2$/NDC and (b) Eu^{3+}/Tb^{3+}@Uio-66-$(COOH)_2$/NDC.

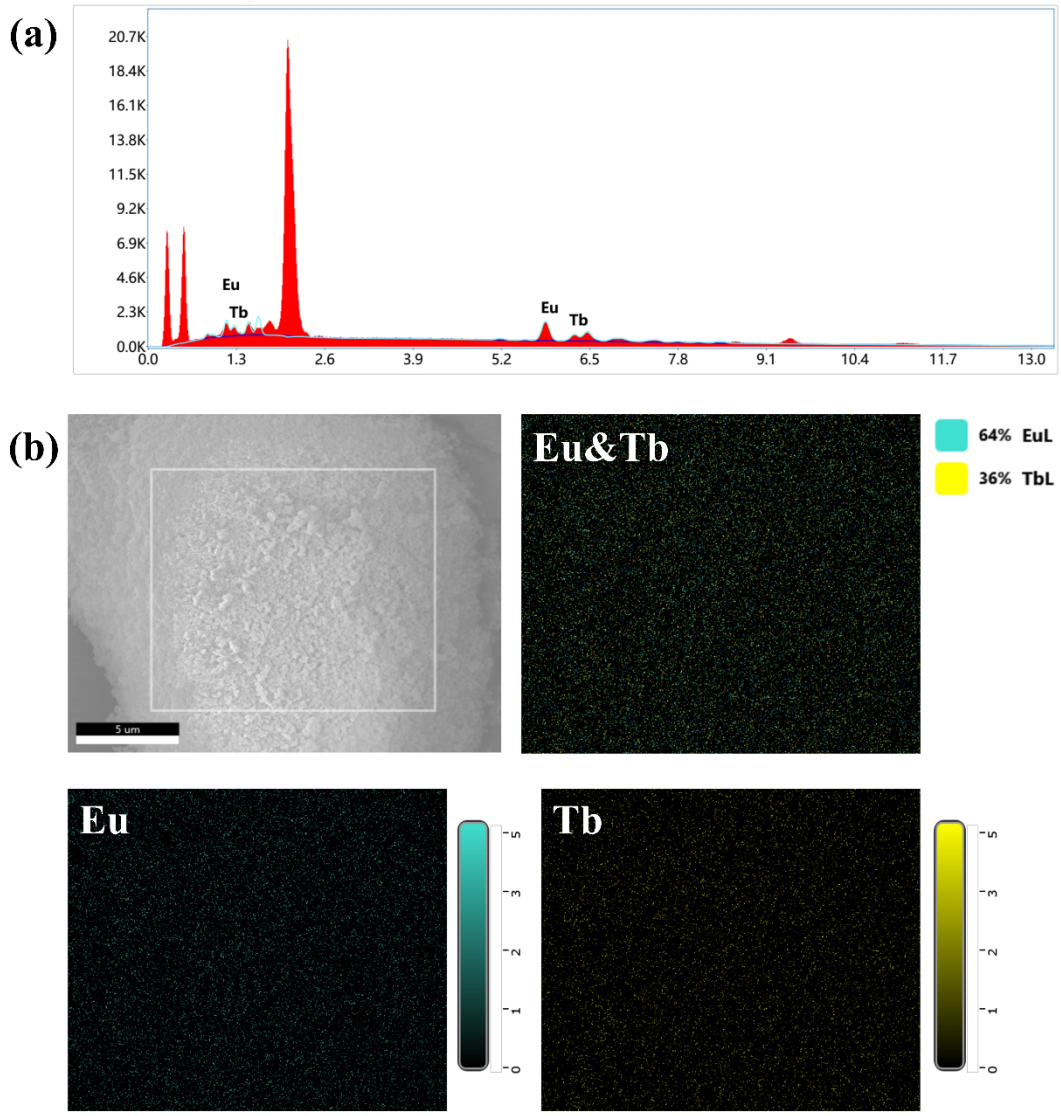

Fig. S4. (a) EDS pattern and (b) EDS mapping of Eu^{3+}/Tb^{3+}@Uio-66-$(COOH)_2$/NDC.

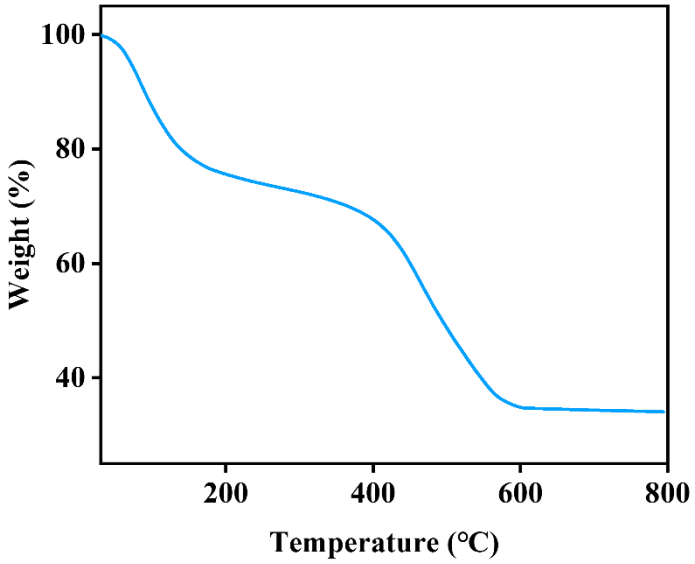

Fig. S5 TGA curve of Eu^{3+}/Tb^{3+}@Uio-66-$(COOH)_2$/NDC.

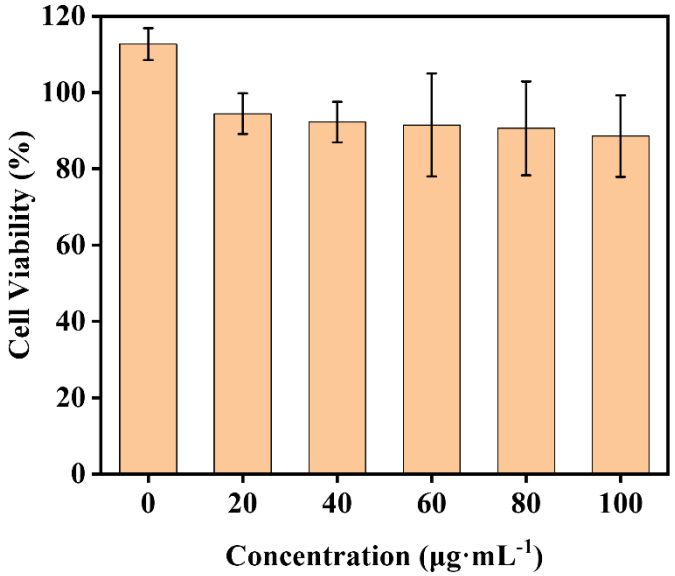

Fig. S6 Cell viabilities of Eu^{3+}/Tb^{3+}@Uio-66-$(COOH)_2$/NDC with different concentrations.

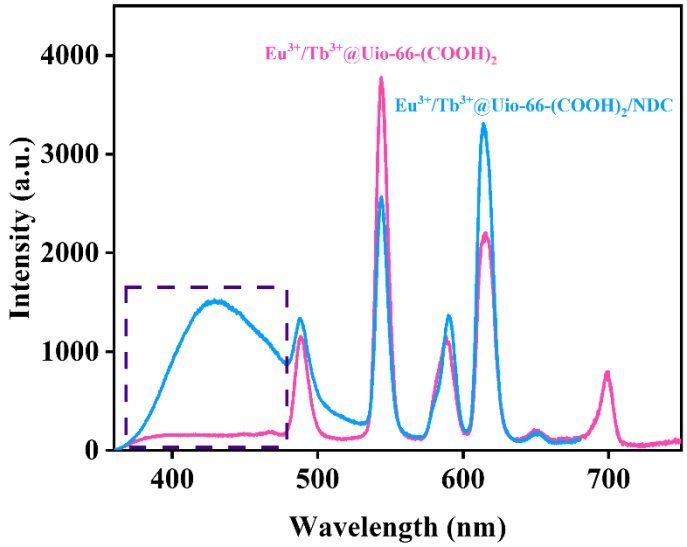

Fig. S7 Emission spectra of Eu^{3+}/Tb^{3+}@Uio-66-$(COOH)_2$ and Eu^{3+}/Tb^{3+}@Uio-66-$(COOH)_2$/NDC under excitation at 325 nm.

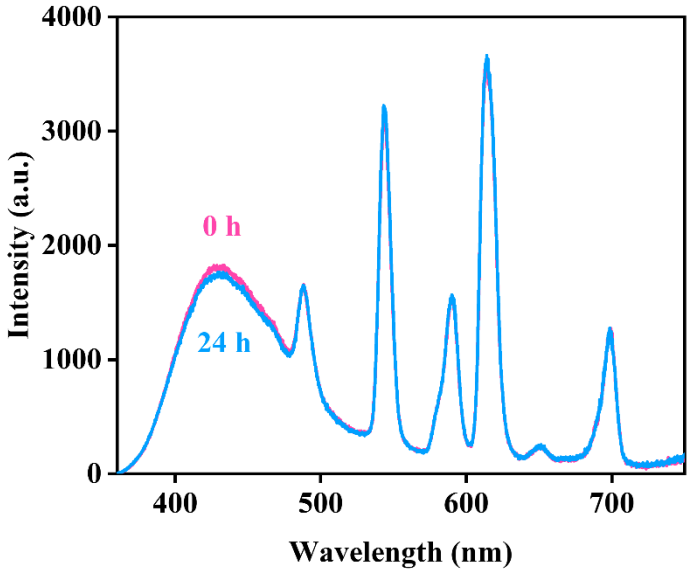

Fig. S8 Emission spectra of Eu^{3+}/Tb^{3+}@Uio-66-$(COOH)_2$/NDC before and after treated with aqueous solution for 24h.

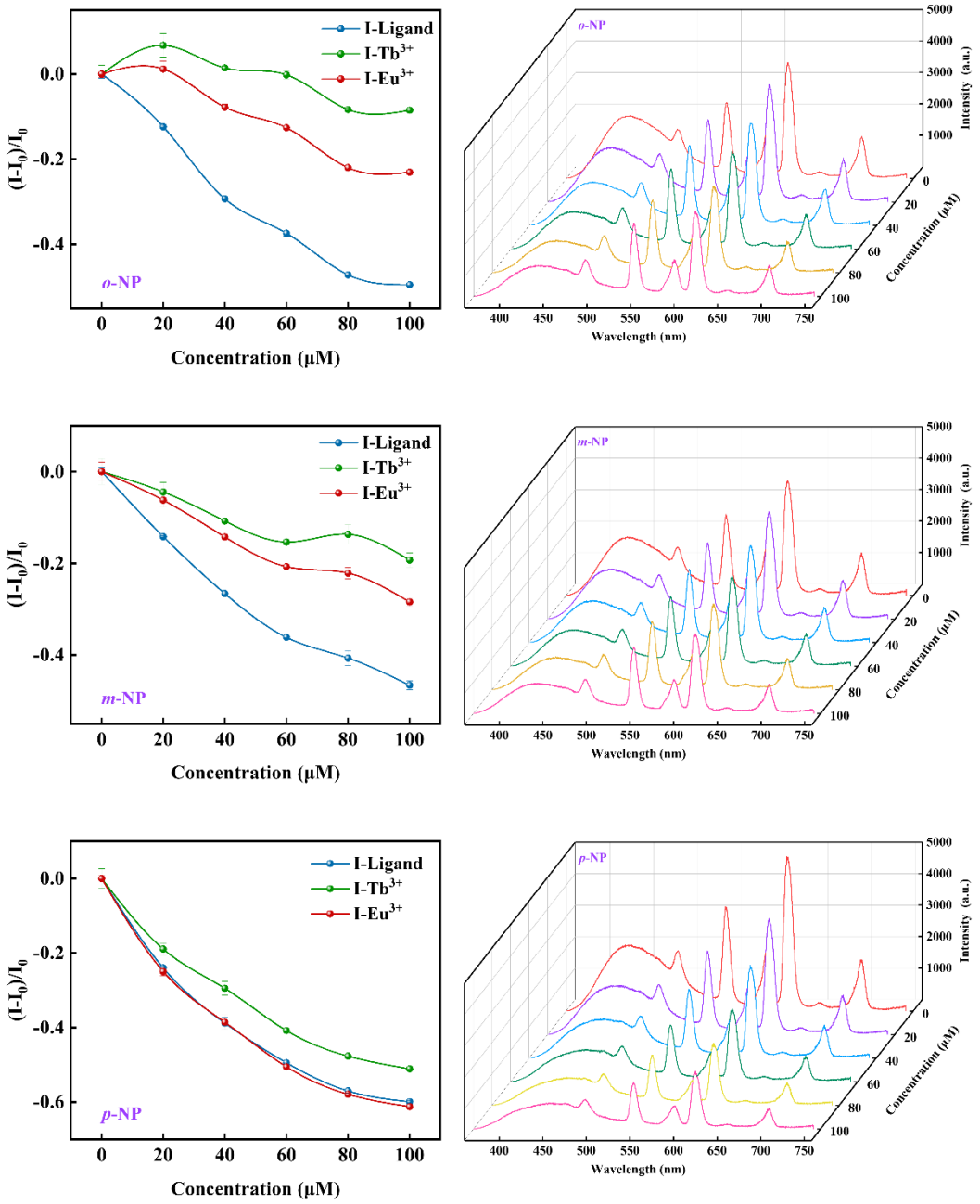

Fig. S9 The fluorescence response of Eu^{3+}/Tb^{3+}@Uio-66-$(COOH)_2$/NDC after exposure to three NPs isomers with different concentrations (0~100 μM) in deionized water.

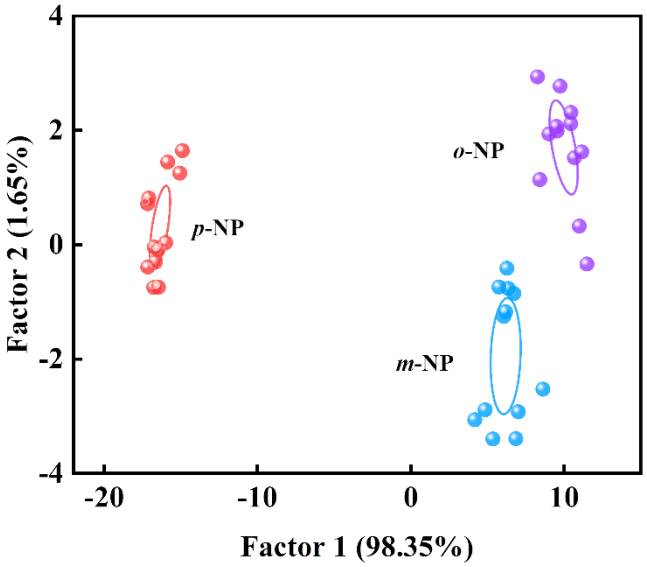

Fig. S10 Canonical score plot of the array sensor response patterns obtained from LDA against three NPs isomers with a concentration of 40~100 μM in deionized water.

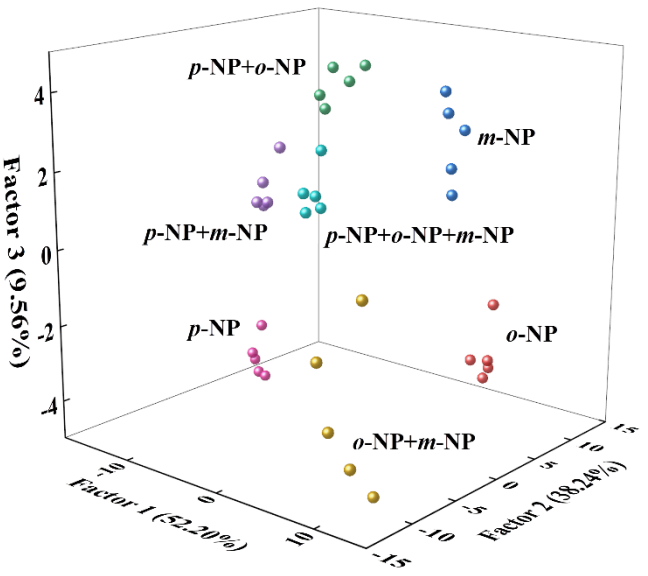

Fig. S11. 3D canonical score plot of the array sensor response patterns obtained from LDA against the binary or ternary NPs mixtures (60 μM for total concentration) in deionized water.

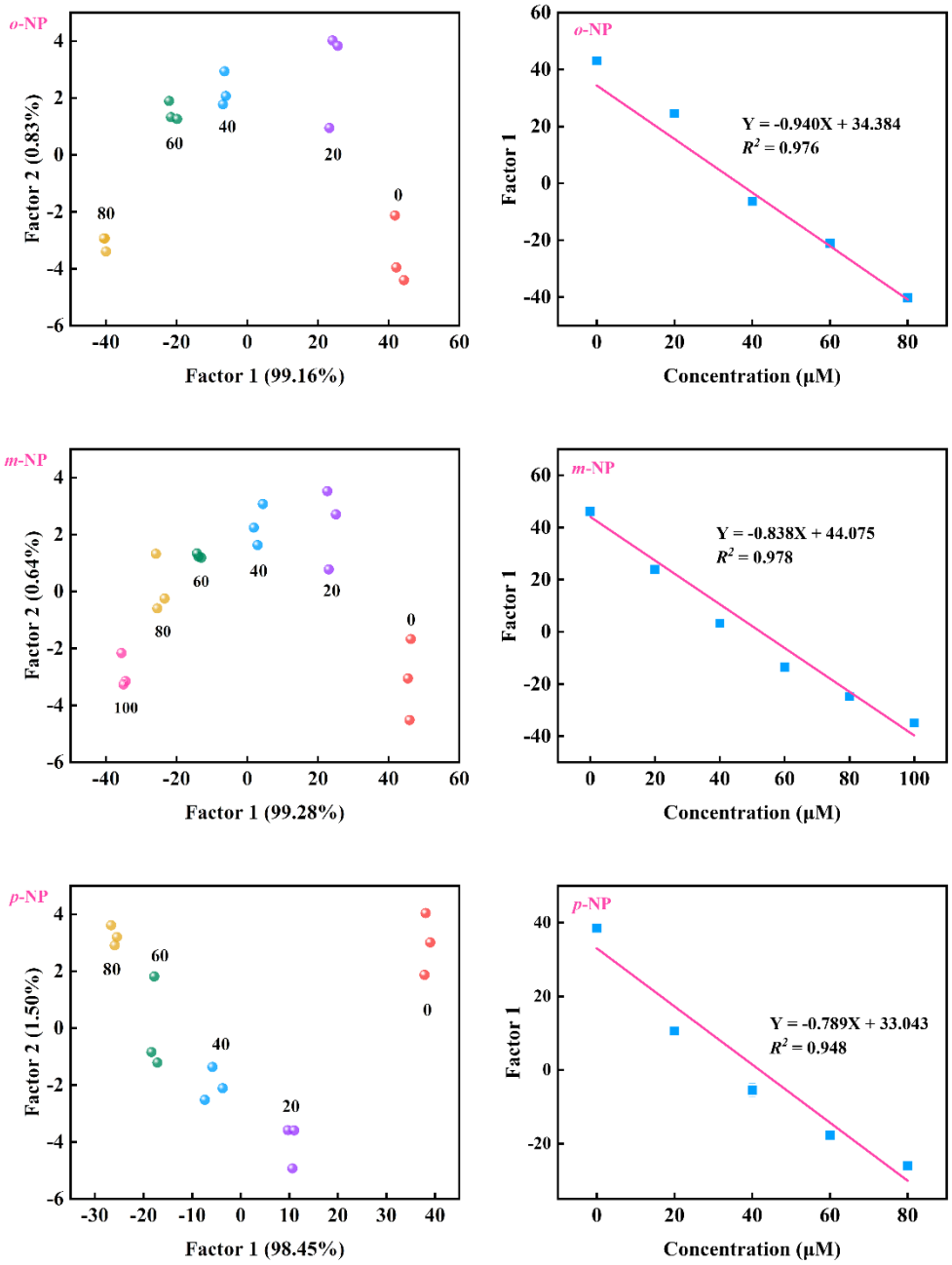

Fig. S12 Canonical score plots and linear regression curves of Eu^{3+}/Tb^{3+}@Uio-66-$(COOH)_2$/NDC sensor array to three NPs isomers with different concentrations.

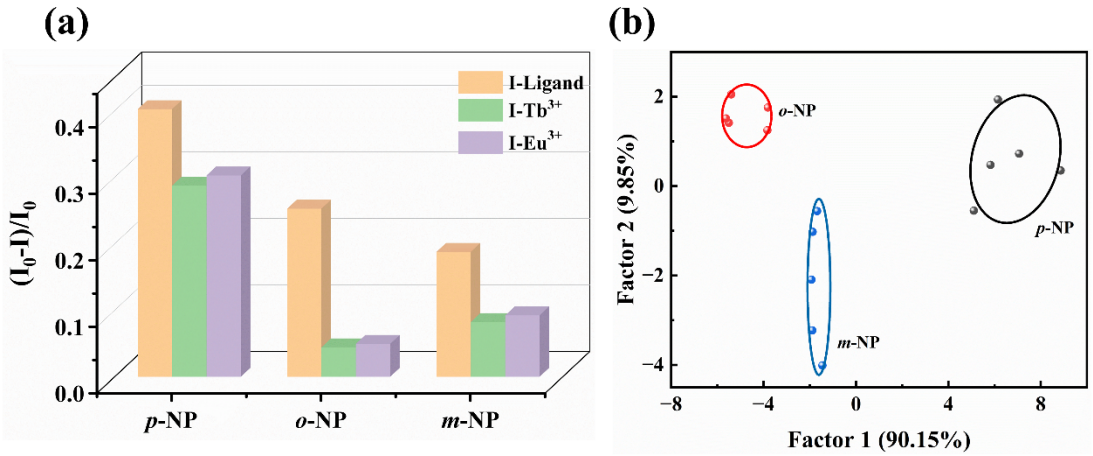

Fig. S13 Canonical score plot of the array sensor (Eu: Tb = 1.81: 1) response patterns obtained from LDA against three NPs isomers with a concentration of 60 μM in deionized water.

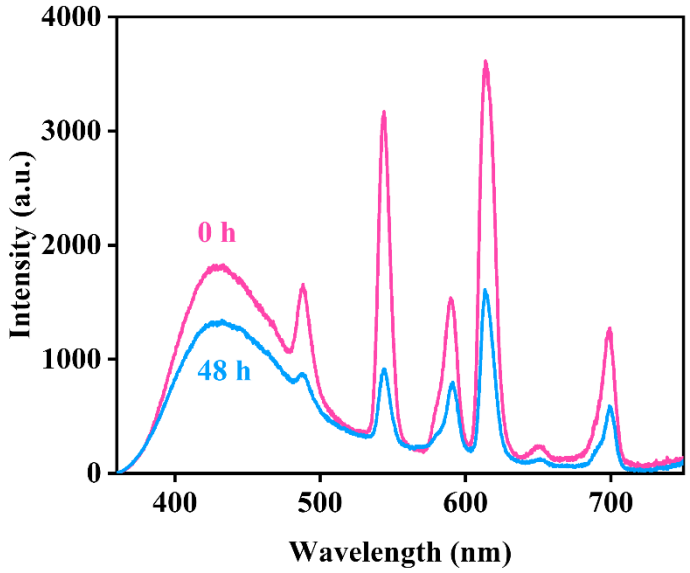

Fig. S14 The fluorescence spectra of the aqueous solution of Eu^{3+}/Tb^{3+}@Uio-66-$(COOH)_2$/NDC before and after standing for 48 hours.

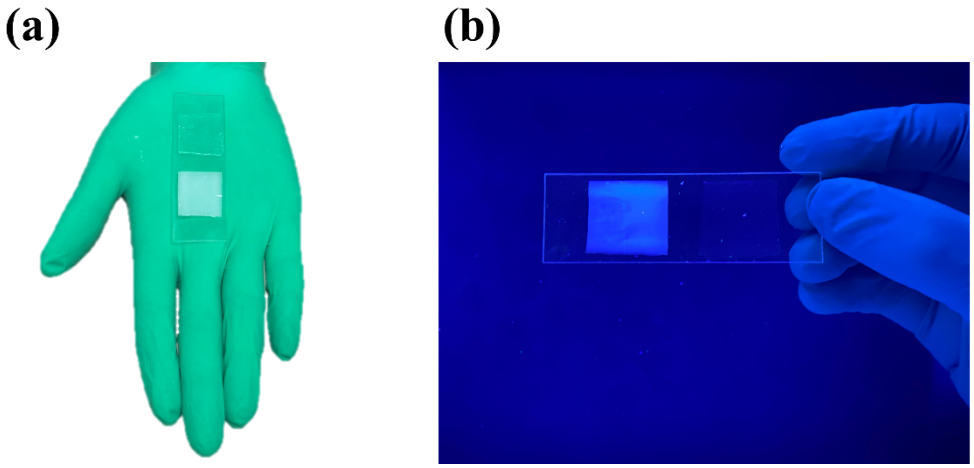

Fig. S15 Physical image of SA hydrogel and LMOF@SA under (a) natural light and (b) 365nm UV lamp.

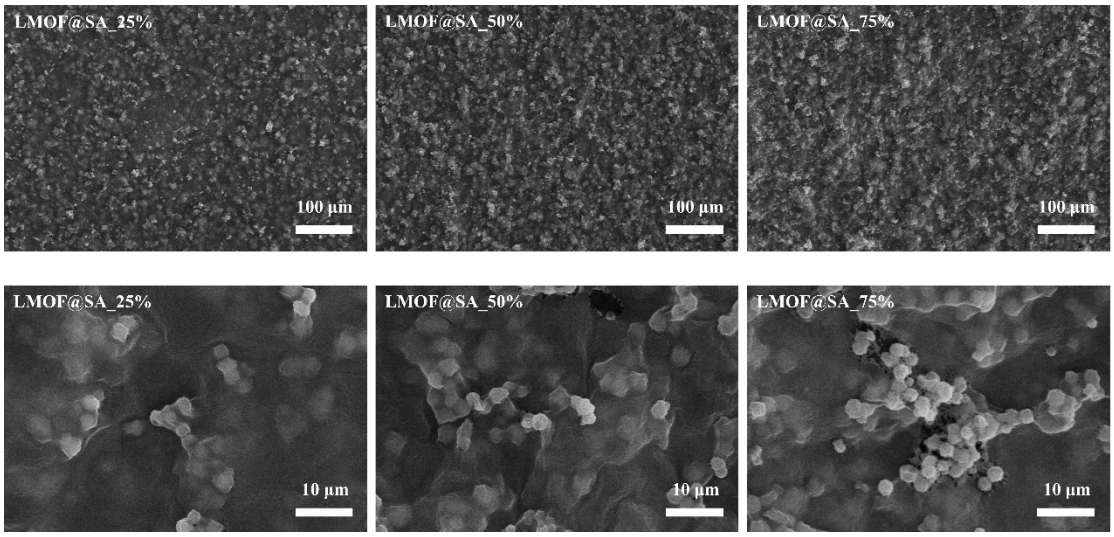

Fig. S16 SEM image of LMOF@SA.

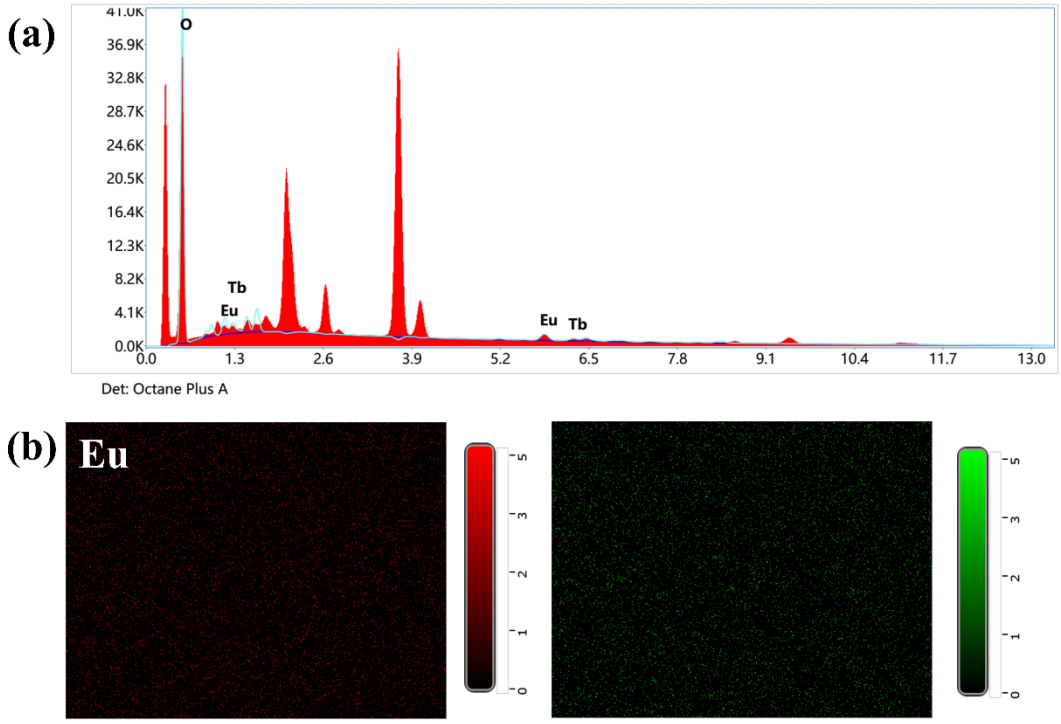

Fig. S17 (a) EDS pattern and (b) EDS mapping of LMOF@SA.

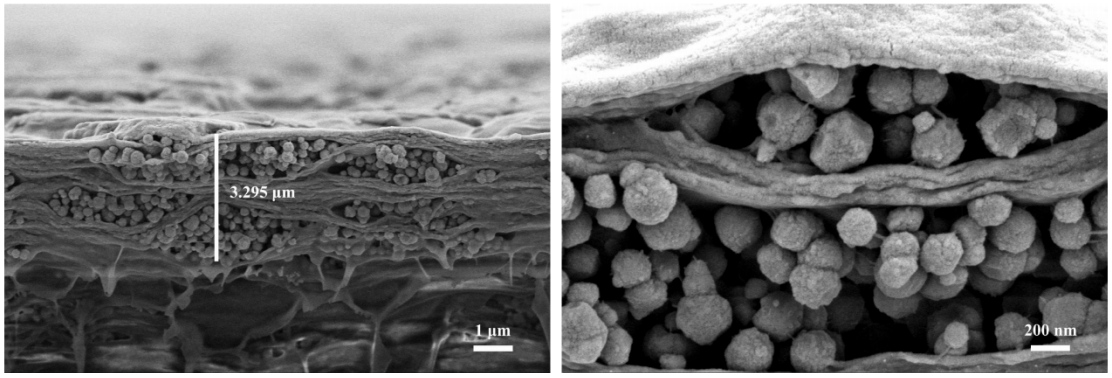

Fig. S18 SEM image of the section of LMOF@SA.

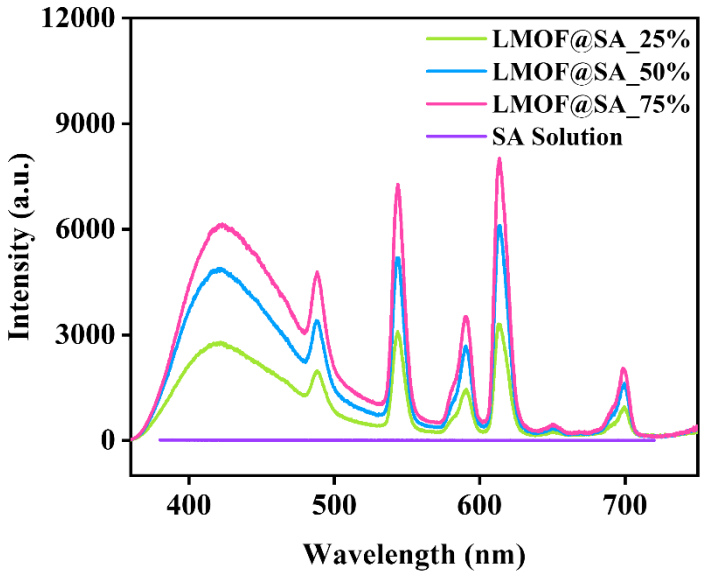

Fig. S19 Emission spectrum of SA solution (50 g·L^{-1}) and LMOF@SA under excitation at 305 nm.

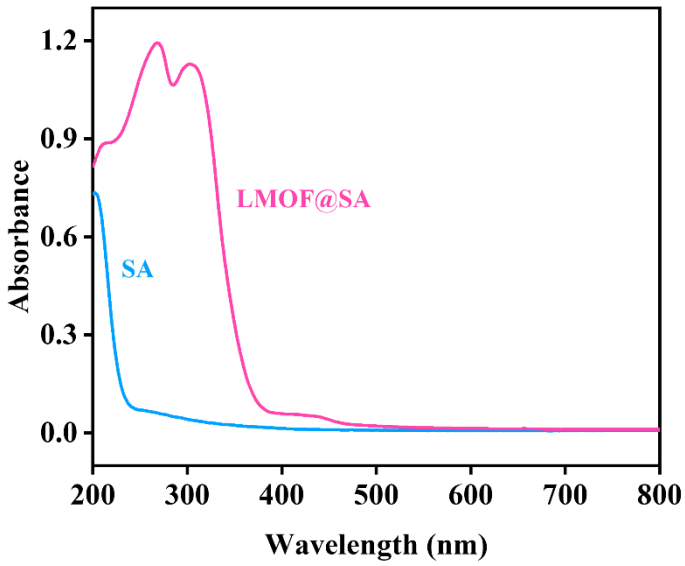

Fig. S20 UV-vis spectra of SA hydrogel and LMOF@SA.

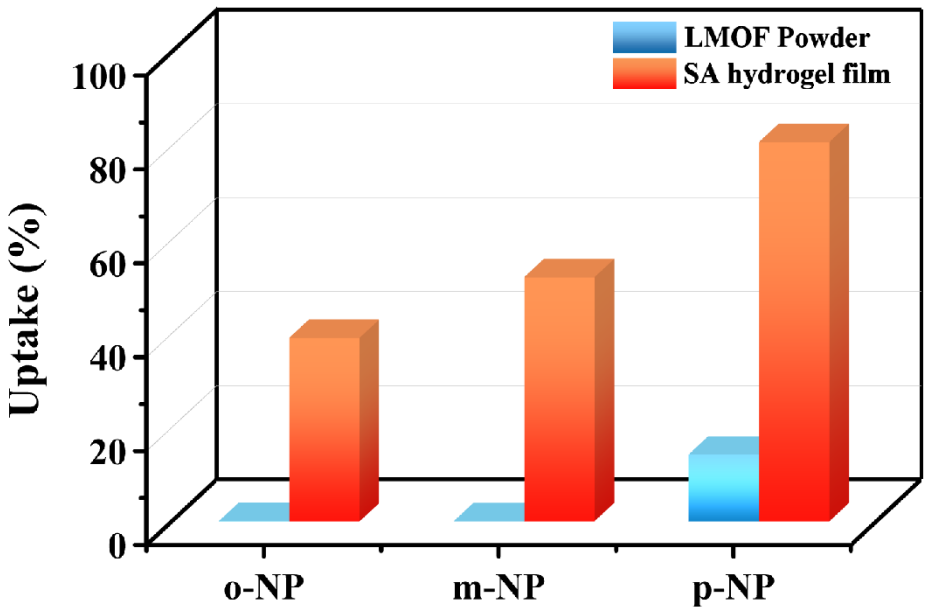

Fig. S21 NPs adsorption ability of powder-form LMOF and SA hydrogel film.

3. Table.

Table S1. Blind test response matrix of Eu^{3+}/Tb^{3+}@UiO-66-$(COOH)_2$/NDC to against three NPs at 60 μM.

Blind samples	$\frac{I - I_0}{I_0}$ **Ligand**	$\frac{I - I_0}{I_0}$ **Tb^{3+}**	$\frac{I - I_0}{I_0}$ **Eu^{3+}**	**Prediction**
p-NP	-0.4918	-0.4075	-0.5035	*p*-NP
p-NP	-0.4999	-0.4147	-0.5111	*p*-NP
p-NP	-0.5035	-0.4146	-0.5149	*p*-NP
p-NP	-0.4962	-0.3935	-0.4983	*p*-NP
p-NP	-0.5053	-0.4053	-0.5109	*p*-NP
m-NP	-0.3659	0.0030	-0.1252	*m*-NP
m-NP	-0.3894	0.0070	-0.1273	*m*-NP
m-NP	-0.4170	-0.0358	-0.1691	*m*-NP
m-NP	-0.4174	-0.0417	-0.1720	*m*-NP
m-NP	-0.4043	0.0048	-0.1349	*m*-NP
o-NP	-0.3615	-0.1522	-0.2066	*o*-NP
o-NP	-0.3536	-0.1291	-0.1930	*o*-NP
o-NP	-0.3812	-0.1253	-0.1979	*o*-NP
o-NP	-0.3820	-0.1156	-0.1899	*o*-NP
o-NP	-0.3854	-0.1071	-0.1885	*o*-NP

Table S2. Blind test response matrix of Eu^{3+}/Tb^{3+}@UiO-66-$(COOH)_2$/NDC with doping ratio 1.81: 1 of Eu^{3+}: Tb^{3+} to against three NPs at 60 μM.

Blind samples	$\frac{I - I_0}{I_0}$ **Ligand**	$\frac{I - I_0}{I_0}$ **Tb^{3+}**	$\frac{I - I_0}{I_0}$ **Eu^{3+}**	**Prediction**
p-NP	-0.4001	-0.2503	-0.2664	*p*-NP
p-NP	-0.4113	-0.2508	-0.2695	*p*-NP
p-NP	-0.4213	-0.2559	-0.2746	*p*-NP
p-NP	-0.4122	-0.2472	-0.2682	*p*-NP
p-NP	-0.4174	-0.2460	-0.2694	*p*-NP
m-NP	-0.1229	0.0779	-0.0827	*m*-NP
m-NP	-0.1037	0.0688	-0.0718	*m*-NP
m-NP	-0.1112	-0.0719	-0.0776	*m*-NP
m-NP	-0.1887	-0.0793	-0.0958	*m*-NP
m-NP	-0.1860	0.0807	-0.0919	*m*-NP
o-NP	-0.2399	-0.0679	-0.0699	*o*-NP
o-NP	-0.2442	-0.0680	-0.0725	*o*-NP
o-NP	-0.2515	-0.0704	-0.0743	*o*-NP
o-NP	-0.2444	-0.0264	-0.0316	*o*-NP
o-NP	-0.2526	-0.0227	-0.0302	*o*-NP